Pulver Benedikt (Orcid ID: 0000-0002-7772-2111)

Auwärter Volker (Orcid ID: 0000-0002-1883-2804)

Pütz Michael (Orcid ID: 0000-0001-6601-6804)

A new synthetic cathinone: 3,4-EtPV or 3,4-Pr-PipVP? An unsuccessful attempt to circumvent the German legislation on new psychoactive substances

Benedikt Pulver[1,2,3], Jan Riedel[4], Folker Westphal[1], Steven Luhn[4], Torsten Schönberger[4], Jan Schäper[5], Volker Auwärter[2], Anton Luf[6], Michael Pütz[4*]

[1]State Bureau of Criminal Investigation Schleswig-Holstein, Forensic Science Institute, Mühlenweg 166, Kiel, Germany

[2]Institute of Forensic Medicine, Forensic Toxicology, Medical Center – University of Freiburg, Faculty of Medicine, University of Freiburg, Albertstr. 9, 79104 Freiburg, Germany

[3]Hermann Staudinger Graduate School, University of Freiburg, Hebelstr. 27, 79104 Freiburg, Germany

[4]Federal Criminal Police Office, Forensic Science Institute, Äppelallee 45, 65203 Wiesbaden, Germany

[5]Bavarian State Bureau of Criminal Investigation, Munich, Germany

[4]Institute of Forensic Medicine, Forensic Toxicology, Medical Center – University of Freiburg, Faculty of Medicine, University of Freiburg, Albertstr. 9, 79104 Freiburg, Germany

[6]Clinical Department of Laboratory Medicine, Medical University of Vienna, Waehringer Guertel 18-20, 1090, Vienna, Austria

*Corresponding author:

Michael Pütz

e-mail: michael.puetz@bka.bund.de

ORCID

0000-0002-7772-2111 Benedikt Pulver

0000-0002-1883-2804 Volker Auwärter

0000-0001-8958-5292 Torsten Schönberger

0000-0001-6601-6804 Michael Pütz

This article has been accepted for publication and undergone full peer review but has not been through the copyediting, typesetting, pagination and proofreading process which may lead to differences between this version and the Version of Record. Please cite this article as doi: 10.1002/dta.3371

Abstract

Synthetic cathinones comprise psychostimulants with desired effects like euphoria, increased vigilance, appetite suppression, and – mainly depending on certain structural features – entactogenic properties. 3,4-EtPV (1-(bicyclo[4.2.0]octa-1,3,5-trien-3-yl)-2-(pyrrolidin-1-yl)pentan-1-one) was first mentioned in an online drug forum in September 2021, where its imminent synthesis was announced. The goal was to produce a legal alternative to the phenylethylamines already banned by the German NpSG. In February and June 2022, two samples labeled with the name and molecular structure of 3,4-EtPV were analyzed. The molecular structure of the obviously mislabeled compound was elucidated and comprehensively characterized within the ADEBAR project. The synthetic cathinone identified differed from the declared 3,4-EtPV by a 3,4-propylene bridge instead of a 3,4-ethylene bridge and a piperidine ring instead of a pyrrolidine ring. The short name 3,4-Pr-PipVP (3,4-propylene-2-(1-piperidinyl)valerophenone) was suggested as a semi-systematic name in collaboration with the European Monitoring Centre for Drugs and Drug Addiction. Herein, the results of the analyses are discussed and will enable forensic laboratories to update their databases quickly and identify 3,4-Pr-PipVP confidently. 3,4-Pr-PipVP is already scheduled under the German NpSG. This study highlights that there are ongoing efforts to deliberately circumvent generic definitions given, e.g., in the German NpSG, and that (unintentional?) mislabeling can be an issue. The end user purchasing substances online can never be sure that the material actually supplied will be the one ordered, and he might receive an illicit drug instead of an uncontrolled one. Furthermore, the purity is always unknown, creating health risks due to unexpected effects and potencies.

Keywords

New psychoactive substances, synthetic cathinones, legislation, structure elucidation, mass spectrometry, mislabeling

1. Introduction

New psychoactive substances (NPS), often distributed as 'research chemicals,' pose a continuous public health threat because they are easily accessible online, and their toxicological properties are widely unknown. NPS comprise many different substance groups, among them synthetic cannabinoids, phenylethylamines, or opioids, which aim to mimic the typical effects of classical illicit drugs, and new variants continuously appear on the drug market.[1–7] Synthetic cathinones make up the second largest group of NPS, with 162 substances monitored by the European Monitoring Centre for Drugs and Drug Addiction (EMCDDA) so far. The number of new cathinones that emerged on the European drug market each year has declined to only six in 2021[8,9]; however, synthetic cathinones have been the most prevalent in the drug market for many years, accounting for approximately 25% of all seizures as well as 65% of the total weight of seized material in 2020.[8] In 2021, three of the six newly notified synthetic cathinones were pyrrolidino-cathinones (PCs) (see Figure 1). Overall, PCs, also called 'pyros' in pertinent online fora, represent one third of the synthetic cathinones monitored by the EMCDDA and tend to be accompanied by a high abuse potential.[10–12] The abuse of PCs, especially at high doses, can lead to adverse effects such as tachycardia, hypertension, convulsions, anxiety, paranoia, psychosis, and memory impairment.[13–15] The pyrrolidine ring increases lipophilicity, likely enhancing blood-brain barrier (BBB) permeability and, therefore, central nervous system activity.[16,17] On the other hand, the β-keto function of synthetic cathinones leads to lower lipophilicity compared to amphetamine derivatives. The high potency of PCs has been demonstrated in various in vitro assays and generally poses a threat of unintentional overdosing.[18,19] The structural element of the indanyl (3,4-propylenephenyl) has been identified in only three synthetic cathinones in 2015 so far (5-BPDi, 5-PPDi, and 1-(2,3-dihydro-1*H*-inden-5-yl)-2-phenyl-2-(pyrrolidin-1-yl)ethanone). Currently, no pharmacological data is available on their pharmacological effects. There have been discussions about presumably mislabeled 3,4-EtPV in online drug fora, and users reported stimulant effects after ingestion of the drug. 5-BPDi and TH-PVP (formally notified by the EWS of the EMCDDA in 2015) are structural isomers that can pose challenges in the discrimination due to the same molecular mass and similar molecular structure.

Structure elucidation and analytical characterization were performed within the project ADBEBAR *plus*[23] utilizing gas chromatography-mass spectrometry (GC-MS), (high resolution-)liquid chromatography-electrospray ionization- mass spectrometry ((HR-)LC-ESI-MS), attenuated total reflection-Fourier-transform infrared spectroscopy (ATR-IR), GC-solid state infrared spectroscopy (GC-sIR), Raman spectroscopy, and nuclear magnetic resonance (NMR) analysis. The analytical data were shared with the EMCDDA at the time of identification.[24]

2. Experimental

2.1. Chemicals and reagents

All solvents and solid chemicals were of the highest grade, but at least p.a. (pro analysi) quality, and 3,4-Pr-PipVP was available as pure solid from a test purchase by the Bavarian State Bureau of Criminal Investigation.

2.2. Gas chromatography-electron ionization-mass spectrometry (GC-EI-MS)

For the generation of the free base, 2 mg of the salt was dissolved in 2 mL of demineralized water and alkalized with one drop of NaOH (5% w/w). The solution was extracted with 2 mL diethyl ether, and the ethereal phase was transferred into a new vial.

GC-EI-MS analysis was conducted on a Finnigan TSQ 8000 triple-stage quadrupole mass spectrometer coupled to a Trace GC Ultra gas chromatograph (Thermo Fisher , Waltham, US) equipped with a fused silica DB-1 column (30 m × 0.32 mm i.d., 0.25 µm film thickness) (Agilent Technologies, Santa Clara, US). Sample introduction was performed using a CTC CombiPAL (CTC Analytics, Zwingen, CH) autosampler. GC parameters of the analysis were as follows: injection volume: 0.5 µL, splitless; injector temp.: 280 °C; carrier gas: helium; flow rate: 1.2 mL/min. The oven temperature program was initially kept at 80 °C for 2 min, ramped to 280 °C at 15 °C/min, and subsequently maintained at the final temperature of 280 °C for 20 min. MS parameters were set as follows: ionization mode: EI = 70 eV; emission current: 50 µA; ion source temp.: 220 °C; scan time: 1 s; scan range: *m/z* = 29–600.

Data analysis was conducted using Xcalibur 4.0 Qual Browser (Thermo Fisher) and the National Institute of Standards and Technology (NIST) MS search program (version 2.3) (NIST, Gaithersburg, US). EI-MS spectra were compared to EI-MS spectra libraries provided by the NIST, the European Network of Forensic Science Institutes (ENFSI), Scientific Working Group for the Analysis of Seized Drugs (SWGDRUG), as well as the designer drug library 2022 (DigiLab, SH, DE) and libraries built in-house. Kovats retention indices (RI) were calculated from the measurement of retention times obtained from the constituents of an n-alkane mixture. The temperature program was as specified above. For calculation, logarithmic interpolation was applied between two consecutive n-alkanes.[25]

2.3. Liquid chromatography-mass spectrometry (LC-MS)

For ESI-MS analysis, 1 mg of the pure solid was dissolved in 10 mL of MeOH and diluted at 1:10. The solution was introduced into the ESI interface via a direct insertion syringe at 3–10 µL/min, depending on the signal intensity observed. The analysis was conducted on a Thermo Velos Pro (linear trap) spectrometer (Thermo Fisher). The mass range of the spectrometer was set to *m/z* 50–2,000 for the full scan. The upper limit of the mass range was adjusted to *m/z*($[M+H]^+ + 50$) for the MS^n experiments (up to MS^4). Wideband and non-wideband collision-induced dissociation (CID) spectra were recorded after fragmentation using helium as collision gas. The collision energy was set at an intensity at which the molecular ion peak was retained at 10% intensity of the base peak. HR-MS/MS data were acquired on a Fusion Lumos with the Orbitrap as the mass analyzer set to 100–1000 *m/z* with helium used as collision gas. ESI parameters were as follows: ion spray voltage 3300 V; sheath gas: 12 L/min; aux gas: 2 L/min; sweep gas: 1 L/min; ion transfer tube temp.: 275 °C; vaporizer temp.: 35 °C.

For the LC-ESI-MS/MS analysis, the mass spectrometer mentioned above was coupled to a Thermo Accela 1250 HPLC chromatograph (Thermo Fisher) equipped with an analytical Aqua C18 column (3 µm, 150 × 2 mm, 125 Å) (Phenomenex, Torrance, US). Chromatographic separation was achieved using mobile phase A, 0.25% formic acid (FA) in water, and mobile phase B, 0.25% FA in methanol, at a flow rate of 100 µL/min with a gradient comprised of 0% B for 3 min, then 0% to 98% B in 14 min, 98% B held for 32 min, and 98% to 0% B in 10 min.

The column temperature was held at 24 °C. MS analysis was performed using a data-dependent top seven method in positive ion mode followed by a top five method in negative ion mode with the full MS, and MS/MS scans acquired at unit resolution. After obtaining a full scan, the seven (respectively five) most intense ion species were automatically chosen as precursors for MS/MS experiments in positive and negative ion modes. Data evaluation was conducted using XCalibur 4.0 (Thermo Fisher) in conjunction with the NIST MS Search program (version 2.3) and spectra compared to in-house libraries.

The LC-IT-MS/MS analysis in Vienna was performed using a Thermo Velos Pro linear ion-trap mass spectrometer (Thermo Fisher) coupled to a Dionex HPLC-System Ultimate DPG-3600RS pump equipped with a Luna Omega PS C18 column (150 × 2.1 mm, 1.6 µm) (Phenomenex). Approximately 5 mg of the sample was dissolved in methanol and centrifuged. A PAL CTC Autosampler (CTC Analytics) was used for automated dilution and injection of 1 µl of the diluted sample solution. Chromatographic separation was achieved using mobile phase C, 10 mM ammonium formiate (pH 4.60), and mobile phase D, acetonitrile (ACN), at a flow rate of 700 µL/min with a starting gradient of 10% D increasing to 90% D in 5 min, 90% D held for 5 min, followed by re-equilibration with 10% D for 2 min. The total runtime was 12 minutes and the column temperature was held at 58 °C. Dionex Chromeleon 6.8 SR14 (Thermo Fisher) was used for instrument control of the HPLC components.

A data-dependent MS/MS analysis was performed for ions presenting a signal value above 500 000 cps acquired in the positive ionization full scan, with CID as activation type (35% normalized collision energy) and helium as collision gas. The mass range of the full scan and the MS/MS scan was set to *m/z* 50 to 800 and *m/z* 50 to 550, respectively. The dynamic exclusion function was activated with a duration of 6 seconds. Temperatures of the ion source heater and of the ion-transfer capillary were both set to 400 °C. The sheath, aux and sweep gas flow rates (in arbitrary units) were set to 65, 50 and 5, respectively. For MS instrument control, data analysis, and reference library search LTQ Tune Plus 2.7 (Thermo Fisher), Freestyle 1.8 (Thermo Fisher) and the NIST MS Search program (NIST) were employed, respectively.

Ultra high-performance liquid chromatography quadrupole time-of-flight single and tandem mass spectrometry (UHPLC-QTOF-MS/MS) data were obtained from a Bruker compact Q-TOF instrument (Bruker Daltonics, Billerica, US) and coupled to a Dionex Ultimate 3000 UHPLC system (Thermo Fisher) equipped with a Thermo Hypersil GOLD column (2.1 × 50 mm, 1.9 µm) (Thermo Fisher). Mobile phase E consisted of aqueous buffer (10 mM NH_4HCO_2, 0.12% formic acid), and mobile phase F was ACN. The column temperature was set at 30 °C, the flow rate was 0.2 mL/min, and data were acquired over the total run time of 49 min. The gradient commenced at 10% F and was held for 2 min, then increased to 90% F over 31 min and returned to 10% F over 11 min. QTOF-MS data were acquired in positive mode scanning from *m/z* 50–1070. QTOF-MS parameters: drying gas temp.: 190 °C, drying gas flow: 6 L/min; nebulizer pressure: 0.9 bar; capillary voltage: 4000 V; collision gas: nitrogen; collision energy: 35 eV. Sodium formate was used for calibration purposes.

The matrix-assisted laser desorption ionization (MALDI)-HRMS experiments were performed using a Thermo Scientific MALDI-LTQ-Orbitrap XL hybrid mass spectrometer (Thermo Fisher). The nitrogen laser of the MALDI source was operated at a wavelength of 337.1 nm, a

repetition rate of 60 Hz and a beam diameter of 80 × 100 μm^2. The MALDI acquisition method consisted of a full scan (scan 1) ranging from 50 to 550 *m/z* followed by a data-dependent MS/MS scan of the most intense ion acquired during scan 1 with dynamic exclusion set to two cycles resulting in 30 scans per sample in total. The spectral resolution was set to 100 000 for both scans. CID was performed using helium as collision gas and a normalized collision energy of 35%. The MALDI experiments were performed with 'survey crystal positioning system' (CPS) selected as plate motion, automatic gain control (AGC) enabled, and automatic spectrum filtering (ASF) disabled. The laser energy was set to 30 μJ.

2.4. Infrared spectroscopy

Attenuated total reflection Fourier-transform infrared spectroscopy (ATR-FTIR) spectra were acquired as solid and neat spectrum using a Nicolet iS20 FT-IR spectrometer with Smart iTX Diamond ATR (Thermo Fisher). Software: OMNIC, Ver. 9.11.706 (Thermo Fisher). The neat IR spectrum was recorded after the following sample preparation procedure: For the generation of the free-base, 2 mg of the salt was dissolved in 2 mL of demineralized water and alkalized with one drop of NaOH (5% w/w). Next, the solution was extracted with 2 mL diethyl ether, the ethereal phase was transferred in a new vial and the solvent was evaporated under a slow nitrogen stream at room temperature until the volume reached approximately 100 μL. Finally, the remaining fluid was aspirated with a glass pipette and transferred directly onto the ATR crystal, where the remaining diethyl ether was continuously evaporated under a stream of nitrogen.

IR spectra were obtained with an Alpha FTIR instrument (Bruker Optics) equipped with a platinum ATR single reflection diamond-sampling module. Approximately 5 mg of the white powder was placed directly onto the ATR sampling module, ensuring that the ATR crystal is entirely covered with the sample, followed by applying sufficient pressure to the anvil by moving the pressure lever in the downward position. Infrared spectra were collected as an average of 24 scans with a wavenumber range of 4000–400 cm^{-1} at a resolution of 4 cm^{-1}. Instrument control and data analysis were carried out using Opus 2.8 (Bruker Optics).

For the acquisition of the solid transmission IR spectrum after gas chromatography, a GC-solid phase-IR-system consisting of an Agilent GC 7890B (Agilent Technologies) equipped with a fused silica capillary DB-1 column (30 m × 0.32 mm i.d., 0.25 μm film thickness), an Agilent G4567A probe sampler (Agilent Technologies) and a DiscovIR-GC™ (Spectra Analysis, Marlborough, US) was used. First, 1 μL of the solution described in Section 2.2 concentrated one-fold was injected onto the column. Then, the eluting substances were cryogenically deposited on a spirally rotating ZnSe disk cooled by liquid nitrogen to −40 °C. Finally, the IR spectra were recorded using a nitrogen-cooled MCT detector through the IR-transparent ZnSe disk.

The GC parameters were as follows: splitless; injection port temp.: 240 °C; carrier gas: helium; flow rate: 2.5 mL/min. Chromatographic conditions were chosen to achieve congruent retention times with the GC-EI-MS analysis: oven temp. program: 80 °C for 2 min, ramped to 290 °C at 20 °C/min, and maintained for 20 min; oven temp.: 280 °C. Infrared conditions: transfer line temp.: 280 °C; restrictor temp.: 280 °C; disc temp.: −40 °C; dewar cap temp.: 35 °C; vacuum: 0.2 mTorr; disc speed: 3 mm/min; spiral separation: 1 mm; wavelength resolution:

4 cm^{-1}; IR range: 650–4000 cm^{-1}; acquisition time: 0.6 s/file; scans/spectrum: 64. Data were processed using GRAMS/AI Ver. 9.1 (Grams Spectroscopy Software Suite, Thermo Fisher) followed by OMNIC Software, Ver. 7.4.127 (Thermo Fisher).

2.5. Raman spectroscopy

Approximately 5 mg of the solid powder was placed onto the teflon septum of an autosampler vial cap. The Raman laser was focused on the sample and Raman data were acquired as an average of 10 consecutive scans acquired through a BAC151B Raman Video Microsampling System (B&W TEK, Plainsboro, US) at 785 and 1064 nm using a BWS465-785S spectrometer and a BWS485-1064S-05 spectrometer, respectively.

2.6. Nuclear magnetic resonance spectroscopy

For analysis of the solid, approximately 1 mg was dissolved in a deuterated solvent. The NMR spectra (1D and 2D spectra) were recorded with an AVANCE III HD 500 spectrometer and a 5 mm BBO Prodigy Cryo probe (Bruker BioSpin). Chemical shifts are reported in ppm relative to TMS ($^{1}H/^{13}C$: d = 0.00) as reference. The compound was fully characterized by 1D- and 2D-NMR spectra by using the following parameters:

1D-^{1}H: single pulse experiment with 90° pulse, 4 scans, relaxation delay 63 s, exponential multiplication with line broadening 0.2 Hz; 1D-$^{13}C\{^{1}H\}$: APT, proton decoupled, 4000 scans, exponential multiplication with line broadening 1.0 Hz; 1D-^{35}C: single pulse experiment, 160 scans, $^{1}H,^{1}H$-COSY: pulse sequence: cosygpqf.3, acquired size (2028, 256), 4 scans, spectral size (4096, 2048), $^{1}H,^{13}C$-HSQC: pulse sequence: hsqcedetgpsp.3, acquired size (1024, 128), non-uniform sampling (sampling amount 25%), 8 scans, spectral size (1024, 1024); $^{1}H,^{13}C$-HMBC: pulse sequence: hmbcetgpl3nd, acquired size (1024, 128), non-uniform sampling (sampling amount 25%), 32 scans, spectral size (1024, 1024); $^{1}H,^{13}C$-H2BC: pulse sequence: hsqcedetgpsp.3, acquired size (1024, 128), non-uniform sampling (sampling amount 25%), 16 scans, spectral size (2048, 1024); $^{1}H,^{15}N$-HMBC: pulse sequence: hmbcgpndqf, acquired size (1024, 128), non-uniform sampling (sampling amount 25%), 16 scans, spectral size (2048, 1024).

The spectra evaluation was performed using MNova V. 14.2 (Mestrelab, Santiago de Compostela, ES). The integrals of the 1D-^{1}H spectrum were defined by the line fitting mode 'qGSD'. The ^{1}H and ^{13}C spectra predictions were performed by using the MNova "NMR Predict" plugin with the "Modgraph NMRPredict Desktop" model with the "fast increments" algorithm. Additionally, the model has been trained by implementing approximately 1500 own, fully assigned spectra of drugs and related substances.

3. Results and discussion

To the authors' knowledge, the first mention of 3,4-EtPV goes back to a post in an online forum in September 2021. The post detailed that a German vendor for 'research chemicals' had been performing experiments and invented new compounds. The disclosed intention of the design

efforts was to circumvent the German NpSG by including the benzocyclobutene group not covered by the definitions so far.

Information on the subsequent synthesis of the alleged 3,4-EtPV is limited. The production of three batches between November 2021 and June 2022 is mentioned, and the compound is supposed to be present as hydrochloride with a molecular mass of the salt of 293.83 g/mol. Online vendors selling research chemicals often advertise their products by presenting data on analytical characterization to assure purity and quality. In this case, the vendor shared analytical data of the first and second batch in the form of ^{1}H-NMR spectra and an ion chromatogram together with a mass spectrum, probably from an LC-MS analysis (see Supporting Information, SI). The mass spectrometric data was inconclusive and did not allow the deduction of the molecular mass of the analyte. One of the ^{1}H-NMR spectra supplied by the online vendor was acquired using DMSO (see SI Figure 26). The signals in the aliphatic region of 0–2 ppm exhibit signals with similar integral values and chemical shifts compared to the NMR spectra of 3,4-PrPipVP. The triplet at 0.8 ppm can likely be assigned to the CH_3 group of the alkyl chain and the multiplet at 1.1 ppm to the adjacent methylene group. The two protons at C4 in the piperidine ring of 3,4-PrPipVP are split into two signals at 1.9 and 1.4 ppm with an integral value of one. The same chemical shifts and integral values can be observed in the NMR spectrum supplied by the online vendor, implying the presence of 3,4-PrPipVP in the sample analyzed by the online vendor. However, ultimately the molecular structure cannot be confirmed without 2D experiments revealing the correlations with other atoms in the molecule.

The synthesis of 3,4-EtPV was described as 'difficult' by the vendor, who probably ordered the substance from a custom synthesis laboratory. The ring structure element defined as 'A' in the NpSG corresponding to the benzocyclobutene ring likely has to be synthesized rather than introduced into the synthesis as an educt. The incorporation of the indanyl element might be the result of unsuccessful attempts to synthesize the bicyclo[4.2.0]octa-1,3,5-triene ring system, leading the supplier to shift to the more common and stable ring system, probably without knowledge of the ordering research chemical vendor.

Similar to the case presented in the present study, the analysis of a sample submitted as 3,4-EtPV in February 2022 was reported in Vienna, Austria.[26] The inconclusive results did not support the identification of 3,4-EtPV at the time. The comparison of the LC-MS/MS and MS^n mass spectra and the IR spectrum acquired of the sample as received are discussed below. Based on the mass spectrometric fragmentation after electrospray ionization and the IR spectrum, 3,4-Pr-PipVP was confirmed to be present in the sample mislabeled as 3,4-EtPV in Vienna.

The current German new psychoactive substances act (German: Neue-psychoaktive-Stoffe-Gesetz, NpSG) includes structural definitions for derivatives from 2-phenylethylamines, synthetic cannabimimetics (also referred to as synthetic cannabinoids), benzodiazepines, 'U compounds' (*N*-(2-aminocyclohexyl)amides like U47700), tryptamines, LSD derivatives, arylcyclohexylamines (analogs of ketamine and PCP) and benzimidazole opioids, ultimately aiming at scheduling most of all circulating NPS on the drug market.[20,21] Both 3,4-EtPV and

3,4-Pr-PipVP are derived from phenylethylamine and, therefore, would be compared to the substance group one of the annex of the NpSG (substances derived from 2-phenylethylamine) to check their conformity/nonconformity to the group definitions of the NpSG. Figure 2 displays a simplified overview of the information contained in the German legislative text of the annex of the NpSG that is based on the 2021 version.[21]

Group one describes compounds derived from the 2-phenylethylamine base structure that are built by combining structural element A, e.g., methylenedioxyphenyl, thienyl, phenyl, indanyl, and structural element B, which defines the substitution of the nitrogen and the α-carbon. Synthetic cathinones with their 2-amino-1-phenyl-1-propanone base structure are a subgroup of the phenylethylamines explicitly mentioned in the legislative text. For synthetic cathinones, the generic structure shown in Figure 2 can be simplified by defining R_5 and R_6 through a ketone and either R_4 or R_3 by a methylene group. 3,4-EtPV and 3,4-Pr-PipVP are synthetic cathinone derivatives as of this definition with a butyl instead of the methyl group for R_4 or R_3. The molecular mass limit of 500 u is not reached in both cases.

The substituents of the nitrogen atom, R_1, and R_2, form a pyrrolidine ring in 3,4-EtPV and a piperidine ring in 3,4-Pr-PipVP. Both heterocycles conform to the definitions of the German NpSG. The substituents R_3 and R_4 contain a hydrogen atom and a C_4 alkyl chain. Because the limit of ten atoms of the alkyl chain is not reached, R_3 and R_4 in 3,4-EtPV and 3,4-Pr-PipVP also conform to the German NpSG. The substitution of the structural element A phenyl in positions 3 and 4 via an ethylene group does not lead to a ring system listed in the definitions of structural element A. Thus, 3,4-EtPV is not scheduled under the NpSG published on November 21, 2016 (Federal Law Gazette I p. 2615), last amended by Article 1 of the Act of July 02, 2021 (Federal Law Gazette I p. 2231)).[20,21] In 3,4-PrPipVP, the structural element A is substituted in positions 3 and 4 via a propylene group which yields a cyclic system fused to the structural element A. The resulting indane bicyclic ring system is defined as structural element A. Therefore, 3,4-PrPipVP does not represent a legal alternative to banned synthetic cathinones.

3.1. Mass spectrometry analysis

Four main peaks were detected in the total ion chromatogram of the GC-EI-MS analysis of the unknown sample as the free base. Additionally, indane, 1-(butenyl)piperidine, and 1-(piperidin-1-yl)butan-1-one were detected in relatively low abundance in the GC-EI-MS analysis. The first peak at a retention time of 10.03 min can be assigned to ionol, a stabilizing agent in the diethyl ether used to extract the free base of the analyte. The second peak at 12.01 min was tentatively assigned to 1-(2,3-dihydro-1*H*-inden-5-yl)pentan-1-one, based on fragmentation after EI ionization and confirmation of the molecular mass of 202 Da by chemical-ionization-MS (CI-MS) analysis and is supposed to be retained as an educt from synthesis. The EI mass spectrum extracted at 12.01 min can be found in the SI.

The third peak at 14.70 min could not be assigned to a molecular structure (the extracted EI mass spectrum can be found in the SI, Figure 2). The main component of the white solid, later identified as 3,4-Pr-PipVp, and the corresponding GC-artifact formed by the loss of 2H are

assigned to the peaks at 15.18 and 15.42 min, respectively. The EI-MS spectra are shown in Figure 3 and the proposed fragmentation pathway of 3,4-Pr-PipVP after EI ionization can be found in the SI.

The white solid was labeled '3,4-EtPV' and the corresponding chemical structure by the vendor. Thus, the base peak of the EI mass spectrum and the molecular ion peak were expected to be at *m/z* 126 and 257, respectively. The molecular ion peak at *m/z* 285, corroborated by CI-MS analysis, suggests an increase of 28 Da of the molecular mass of the unknown compound compared to 3,4-EtPV. The base peak at *m/z* 140 allows the suggestion that either the amine or the side chain contains an additional methylene group. The second methylene group is most likely included in the corresponding neutral loss fragment leading to the base peak. It thus contradicts the presence of the cyclobutene benzyl structural element that is pivotal for the legal status. The detection of 1-(2,3-dihydro-1*H*-inden-5-yl)pentan-1-one corroborates the assumption that the unknown compound contains an indanyl element.

Shared with the PC 5-BPDi, the fragment ion assigned to the base peak at *m/z* 140. After inductive cleavage at the carbonyl group of 3,4-Pr-PipVP, further fragmenting into the product ion at *m/z* 55 occurs. The σ-cleavage of the C_3 alkyl chain from fragment ion at *m/z* 140 yields the fragment ion at *m/z* 98. For comparison, in the EI mass spectrum of the PC 5-BPDi, the fragment ion at *m/z* 84 is formed. The molecular ion (*m/z* 285) and fragment ions at *m/z* 140, 98, 84, and 55 exhibit dehydrogenation and yield -2H peaks at 283, 138, 96, 82, and 53. After the loss of the C_3 alkyl side chain, dehydrogenation was still observed. Thus, the most likely site of unsaturation produced upon injection and after EI ionization is located in the pyridine ring system. The exact unsaturation position is unknown and cannot be deduced from the mass spectrum. The increased intensity of the fragment ion at *m/z* 84 in the EI mass spectrum of the GC-artifact further corroborates the assignment of the double bond to the heterocycle. The aryl acylium ion at *m/z* 145, less stable in indanyl than the methylenedioxy analogs, can be formed after α-cleavage at the carbonyl group, and subsequent neutral loss of CO and deprotonation yield ions at *m/z* 117 and 115, respectively.

In the synthetic cathinone bk-IVP (1-(2,3-dihydro-1*H*-inden-5-yl)-2-(ethylamino)pentan-1-one), McLafferty rearrangement and loss of ethylamine led to a fragment ion at *m/z* 202.[27] This fragmentation is not possible in 3,4-Pr-PipVP due to the heterocycle. Other synthetic cathinones in which the substituents of the nitrogen atom form a ring system will likely miss the corresponding product ions after EI ionization as well. The GC artifact of 3,4-Pr-PipVP formed upon fragmentation contains an additional double bond formed by the loss of H_2. The position can be located within the pyridine ring. The intensity of the iminium ion at *m/z* 84 is increased in the artifact. Additional fragment ions containing the pyridine ring show the loss of 2 Da: 242→240, 140→138, and 98→96.

The analytical differentiation of synthetic cathinones with similar structural features or the same molecular mass can be challenging. The PCs 5-BPDi, 5-PPDi, and 1-(2,3-dihydro-1*H*-inden-5-yl)-2-phenyl-2-(pyrrolidin-1-yl)ethanone differ from one another through the substitution in α-position to the pyrrolidine ring. The EI mass spectra of 5-BPDi and 3,4-Pr-

PipVP are highly similar. The differences are limited to the intensity of fragment ion at *m/z* 84 and the fragment ions formed after the loss of the alkyl side chain in 3,4-Pr-PipVP and 5-BPDi at *m/z* 242 and 228, respectively. The EI mass spectra of 5-PPDi and 1-(2,3-dihydro-1*H*-inden-5-yl)-2-phenyl-2-(pyrrolidin-1-yl)ethanone are more easily distinguished by the base peak at *m/z* 112 and *m/z* 160, respectively. The structural isomers TH-PVP and 3,4-Pr-PipVP can be distinguished via two diagnostic fragment ions. The inductive cleavage at the β-ketone in TH-PVP yields the base peak at *m/z* 126, and α-cleavage yields the fragment ion at *m/z* 156, both different from *m/z* 140 and 145 produced upon EI of 3,4-Pr-PipVP. The use of a category A analytical method[28] (e.g., IR; Raman or NMR) in addition to EI-MS is highly advisable, as demonstrated by this case.

(+)-ESI MS^n and MS/MS mass spectra were acquired on a linear ion trap instrument (Q_{IT}) using resonance excitation collision-induced dissociation (RE-CID) and a QTOF mass analyzer utilizing ion beam (IB)-CID, respectively. No negative ion mode mass spectra were accessible. The different excitation techniques lead to different fragment ions, as highlighted in Table 2. Fragmentation on the IT mass spectrometer yields product ions of higher masses with lower energies. The excitation in the QTOF instrument allows the fragmentation along high-energy pathways like the loss of the alkyl radical $C_3H_7^{\bullet+}$ forming an-odd electron fragment ion at *m/z* 243.1616 ($C_{16}H_{21}NO^{\bullet+}$). Notably, all fragment ions identified on the Q_{IT} instrument were also observed using the QTOF mass analyzer, with some ions only detected as minor fragments at low intensities (see Figure 4). Both MS/MS mass spectra of 3,4-Pr-PipVP exhibit the same, most abundant peaks at *m/z* 201, 131, 140, and 145. The higher collisional energy used for acquiring the HR-MS/MS data leads to more intensity in the low *m/z* region, and fragment ions at higher *m/z* were observed with lower intensity when compared to the Q_{IT} MS/MS mass spectrum (see Figure 4).

The spectral differences are influenced by the number of collisions, the time window of activation, and the transferred energy. The quadrupole collision cell of the QTOF instrument can be operated at higher pressure due to the effect of collisional focusing in the RF collision cell resulting in more extensive dissociation without loss of signal intensity. The activation time scale of 0.5-1 ms, together with high collision energies, allows the observation of high-energy fragmentation processes. CID in a trapping instrument has to be performed at lower collision energies to avoid ejection of the trapped precursor ions. Several hundred collisions are required to increase the internal energy of the precursor over a longer time scale of 10 – 100 ms. Furthermore, only the precursor ion is excited in resonance excitation CID through its characteristic frequency of motion, whereas in ion-beam CID, fragment ions also collide with the collision gas leading to sequential dissociation.[29,30]

The most stable ions formed after fragmentation of 3,4-Pr-PipVP using IB-CID at 40 eV retain the indanyl piperidinyl structural elements. The 5-methyl indanyl cation can be assigned to the base peak, with the indanyl acylium ion as the second most prominent. The neutral loss of the indane aldehyde yields a fragment ion at *m/z* 140, subsequently fragmenting further, forming the piperidinyl iminium ion at *m/z* 98. The product ions retaining the piperidinyl moiety at *m/z* 140 were also detected on the $Q_{IT;}$ further fragmentation to *m/z* 98 requires an additional MS^n experiment. The odd-electron product ion at *m/z* 243 was not detected on the Q_{IT} instrument.

In contrast, the water loss was not observed in the analysis on the QTOF instrument to a significant degree. The MS/MS spectrum of 5-BPDI, differing from 3,4-Pr-PipVP only in the length of the alkyl side chain, reported by Błażewicz et al. was recorded at 22.2 eV. Thus, it displays fewer product ions in the low *m/z* range. Diagnostic for 3,4-Pr-PipVP is the product ion at *m/z* 201; all other major features are the same. Higher CE voltages would lead to an additional differentiating product ion at *m/z* 84 for the pyrrolidine iminium ion.[30] The proposed fragmentation pathway for the QTOF MS/MS mass spectrum can be found in the SI.

The sample submitted for analysis in Vienna was analyzed using LC-MS/MS on a trapping as well as a MALDI-orbitrap instrument. The four most prominent peaks in the MS/MS spectrum (see in SI Figure 7) acquired on the orbitrap instrument of the precursor ion (*m/z* 286.2) at 35 eV from the unknown sample in Vienna are the same compared to the mass spectrum shown in Figure 4. The molecular mass and composition of 286.2165 Da and $[C_{19}H_{28}ON]^+$, respectively of the precursor ion were confirmed via the $[M+H]^+$ ion species, and further MS^3 fragmentation of the base peak at *m/z* 131 yields the tropylium ion at *m/z* 91 (data not shown). The IT MS^2 mass spectrum of the precursor ion at *m/z* 286 is also in agreement with the IT MS^2 mass spectrum acquired of the NMR confirmed sample.

MS^n experiments were carried out to elucidate the fragmentation pathway and enable consecutive reaction monitoring approaches to identify 3,4-Pr-PipVP. Based on the intensity of the product ions and the structural information accessible, transitions 286→201→131 and 386→140→98 are suitable for the detection of 3,4-Pr-PipVP using MS^n experiments (see Figure 5). All MS^n spectra acquired on 3,4-Pr-PipVP are displayed in the SI Figure 6. The MS/MS mass spectrum of the precursor ion at *m/z* 286 is congruent to the mass spectrum acquired on the IT instrument in Vienna. The product ion at *m/z* 131 is highly stable after RE-CID as it is already formed when the precursor ion is fragmented. Additionally, several other MS^n stages yield *m/z* 131, e.g., the MS^5 mass spectrum of the precursor at *m/z* 145. The bond between the ketone and its α-carbon is less prone to cleavage when applying RE-CID compared to IB-CID, leading to more fragment ions with sequential dissociation of the side chain in the MS^n mass spectra.

Two possible molecular compositions can be proposed at several stages of the fragmentation pathway elucidated on the Q_{IT} instrument. Product ions at *m/z* 183, 173, 159, 155, 145, and 141 can either retain the carbonyl oxygen or comprise a longer alkyl chain. The HR-MS data from the QTOF analysis was used to unequivocally elucidate the molecular composition of all but the product ion at *m/z* 173. Both fragment ions at *m/z* 173.1312 and 173.0959 were observed in the HR-MS/MS mass spectrum resulting from the neutral loss of CO and C_2H_4, respectively. If both product ions are formed upon RE-CID fragmentation of the precursor ion at *m/z* 201, the resolution power of the linear ion trap would not be sufficient to distinguish both ions. Because the oxonium ion at *m/z* 145 is a result of the fragmentation of the ion at *m/z* 173, $[C_{12}H_{13}O]^+$ was tentatively assigned to *m/z* 173. Davidson et al. have also observed both the neutral loss reactions in a study on the fragmentation of the synthetic cathinone α-PVP and other pyrovalerone cathinones. By means of heavy atom labeling, they were able to show that after the loss of the piperidyl moiety and formation of a product ion at *m/z* 161, the neutral loss of CO and C_2H_4 are competing fragmentation pathways. The synthetic cathinones α-PVP and 3,4-Pr-PipVP fragment in a similar manner due to the similar molecular composition of a

heterocycle attached to a pentanone moiety. The added propylene bridge does not influence the formation of fragment ions at *m/z* 173 and 159, which can be corroborated by a heavy atom labeling study by Davidson et al. .[32]

The carbonyl oxygen is eliminated through the loss of water in the transitions 286-268, 201-183, and 159-131. All product ions were detected at low intensities in the HR-MS/MS mass spectrum, which confirms the molecular composition, particularly the absence of oxygen. After the neutral loss of water in the transitions 286-268 and 201-183, the alkyl side chain undergoes stepwise fragmentation, and deprotonation in the indanyl moiety can be observed.

In many cases where deprotonation occurs, multiple locations for the double bond can be postulated: the piperidine ring, the alkyl side chain, and the propylene bridge in the indane moiety are prominent positions where deprotonation is possible. For example, dehydrogenation at the indane moiety is possible, highlighted by the MS^5 mass spectrum of the precursor ion at *m/z* 117 and the MS^3 spectrum of the precursor ion at *m/z* 131. In other cases, the dehydrogenation is more likely located at the alkyl side chain or the piperidinyl ring, e.g., in *m/z* 224, 201, and 183.

The synthetic cathinone TH-PVP is isobaric to 3,4-Pr-PipVP. TH-PVP contains a pyrrolidine heterocycle and a butylene bridge attached to the phenyl moiety. The fragmentation of TH-PVP is analogous to 3,4-Pr-PipVP, and several characteristic fragment ions are formed in the EI-MS and MS/MS spectra. Because most fragment ions contain only either the alkyl bridge or the heterocycle, differentiation between 3,4-Pr-PipVP and TH-PVP is straightforward. See SI Figure 4 for the EI mass spectrum of TH-PVP.

3.2. Infrared spectroscopy analysis

IR spectra of 3,4-Pr-PipVP were acquired from the white solid containing the hydrochloride, and from the free base as neat film and solid after chromatographic separation with accumulation and flash-freezing at −40 °C on a ZnSe disc. The IR solid spectrum of the salt shows a broad absorption band from 2800 to 2000 cm^{-1} due to the interactions of the analyte with the chloride ions (see Figure 6). The IR spectra of the free base exhibit several distinct differences from the solid IR spectrum and cannot be compared directly. The condensed-phase IR spectrum of the free base and the neat IR spectrum are congruent and indicate the high purity of the seized sample. The closest match (but with apparent deviations) found in the database was to the IR spectrum of the free base form of 5-BPDi reported by the Spanish Focal Point in 2016.[9]

Structural differences in the IR spectra of 5-BPDi and 3,4-Pr-PipVP are limited to additional methylene groups in the aliphatic heterocycle and the aliphatic chain of the ketone. Methylene groups absorb in the region of 2960–2850 cm^{-1} due to C-H stretching modes and in the region around1460 cm^{-1} due to the C-H deformation modes. Additionally, the region around 1250–1050 cm^{-1} helps distinguish 5-BPDi from 3,4-Pr-PipVP due to additional out-of-plane deformation modes of the cyclic and acyclic CH_2 groups. The absorption bands at ~1679 cm^{-1}

can be assigned to the C=O stretching absorption of an aryl ketone and the band at 1606 and 1572 cm^{-1} to the symmetric and asymmetric stretching vibration of the conjugated C=C bond. All three bands are stable in intensity and location with only a slight redshift in 5-BPDi compared to 3,4-Pr-PipVP.[33–36]

The solid IR spectrum of the second sample analyzed in Vienna and the solid IR spectrum of the hydrochloride salt of 3,4-Pr-PipVP are congruent, and the overlay of both spectra is shown in SI Figure 12. Therefore, together with the identical (+)ESI-MS/MS mass spectra, the presence of 3,4-PrPipVP in the second sample was confirmed. In addition to the IR spectra, Raman spectra were acquired of the new synthetic cathinone 3,4-Pr-PipVP. The 785 and 1064 nm Raman spectra can be found in the SI and could provide the capability for customs laboratories with mobile Raman instruments to detect 3,4-Pr-PipVP on site.

3.3. Nuclear magnetic resonance spectroscopy analysis

GC-EI-MS, LC-ESI-MS, and IR analysis led to the proposed structure of 3,4-Pr-PipVP. Ultimately, NMR analysis was used to confirm the structure proposed by previous analytical findings. An overview of the chemical shifts, multiplicity, and coupling constants of the ^{13}C and ^{1}H NMR signals of 3,4-Pr-PipVP measured in DMSO-d_6 are displayed in Table 1. The full ^{1}H and the ^{13}C spectra, as well as spectra showing only the signals assigned to the analyte are supplied in the SI, and electronic files of the spectra can be downloaded from the NPS Data Hub (www.nps-datahub.com).

The ^{1}H spectrum of the compound contains 15 signals (28 protons) belonging to the compound. The propionate chain can be identified by combined evaluation of the ^{1}H NMR, ^{1}H,^{1}H-COSY, and ^{1}H,^{13}C-HSQC spectra. The side chain is connected to a CH group split into a multiplet (5.34 ppm). Other signals in the range of 0.8 to 3.6 ppm indicate two aliphatic ring systems in the molecule. The three aromatic signals (8.0 to 7.4 ppm) indicate a typical signal splitting for an 1,3,4 substituted phenyl ring.

In the ^{13}C spectra, 13 signals (19 carbon atoms) can be observed. With the 1D-$^{13}C\{^{1}H\}$APT and the ^{1}H,^{13}C-HSQC spectra, all protonated carbons could be assigned to the corresponding atoms. One CH_3, 10 CH_2, and four CH carbon atoms can be identified. All four remaining signals are quaternary carbons. The one at 197 ppm can be identified as a carbonyl signal due to its chemical shift. With the HMBC correlations, all atoms can be connected by interpreting the cross-peaks. In particular, the correlations prove that the phenyl ring is substituted by the propane chain in positions three and four. The observed HMBC and COSY correlations between the CH_2 protons confirm the pyridine ring. Through 1D-^{35}Cl spectra (acquired in D_2O), chloride has been detected and proves the salt form of the molecule.

4. Conclusion

The present study describes the first identification of the new synthetic cathinone 3,4-Pr-PipVP featuring a piperidyl ring (Pip), a propylene bridge (3,4-Pr), and a valeroylphenone (VP) structural element. The BBB permeability and potency of 3,4-Pr-PipVP are expected to be

similar to 5-BDPI, and discussions in online drug fora on mislabeled '3,4-EtPV' seem to confirm the stimulant properties of this compound. The identification of 3,4-Pr-PipVP in Germany and the analytical data acquired were notified to the EMCDDA and uploaded to the NPS Data hub (www.nps-datahub.com). The analytical data will enable other forensic practitioners to identify this new synthetic cathinone confidently and quickly.

The white solid material was received in a transparent zip-lock bag mislabeled with the molecular structure, molecular mass, and name of 3,4-EtPV. A second sample with the same labeling was submitted for analysis in Vienna. The identification of 3,4-Pr-PipVP in the second sample was based on the mass spectrometric fragmentation in the (+)ESI-MS/MS mass spectra, which are identical to those of the NMR-confirmed sample. The detection of the identically mislabeled research chemical outside of Germany highlights the cross-border availability and affirms the necessity of the timely exchange of valid analytical data to keep pace with the dynamic of the NPS market.

The congruence of the hydrochloride IR spectra unequivocally confirmed the presence of 3,4-Pr-PipVP in the second sample in Vienna, together with the matching mass spectrum. The use of two orthogonal techniques, e.g., MS and IR spectroscopy, should be the standard procedure to ensure the differentiation of a compound from other structurally related NPS. The challenge of the extensive chemical diversity of NPS can be overcome by laboratories with limited equipment, i.e., no NMR instrument, through the application of the analytical data provided in the NPS Data Hub.

Analytical data shared by the online vendor did neither allow the assessment of the molecular structure nor the deduction of the claimed purity of 98%. The structural element pivotal for the circumvention of the German NpSG was not present, likely due to difficulties during synthesis. The present case once again points to the issue many consumers inevitably face when purchasing supposedly "legal" alternatives to scheduled drugs. Vendors may – knowingly or unknowingly – label their products as legal alternatives even if the actual active ingredient is already controlled under current legislation. In this case, the newly identified synthetic cathinone 3,4-Pr-PipVP is already scheduled under the NpSG in Germany, and no amendment of the substance groups is necessary. On the one hand, the failed attempt to produce and market the cathinone 3,4-EtPV highlights the ongoing efforts to circumvent the generic definitions given by legislations like the German NpSG. Furthermore, it shows that this goal is increasingly difficult to reach because the generic definitions might eventually leave only those variants unscheduled, which are either without psychotropic activity or not accessible via chemical synthesis with reasonable effort.

2.1. Declaration of interests

The authors declare no competing financial interests.

2.2. Acknowledgments

This publication was co-funded by the Internal Security Fund of the European Union (grant no.: IZ25-5793-2019-33).

5. References

1. Deventer MH, Van Uytfanghe K, Vinckier IMJ, Reniero F, Guillou C, Stove CP. Cannabinoid receptor activation potential of the next generation, generic ban evading OXIZID synthetic cannabinoid receptor agonists. *Drug Test Anal*. Published online May 22, 2022:dta.3283. doi:10.1002/dta.3283

2. Deventer MH, Van Uytfanghe K, Vinckier IMJ, Reniero F, Guillou C, Stove CP. A new cannabinoid receptor 1 selective agonist evading the 2021 "China ban": ADB-FUBIATA. *Drug Test Anal*. n/a(n/a). doi:10.1002/dta.3285

3. Halter S, Pulver B, Wilde M, et al. Cumyl-CBMICA: A new synthetic cannabinoid receptor agonist containing a cyclobutyl methyl side chain. *Drug Test Anal*. 2021;13(1):208-216. doi:10.1002/dta.2942

4. Haschimi B, Grafinger KE, Pulver B, et al. New synthetic cannabinoids carrying a cyclobutyl methyl side chain: Human phase I metabolism and data on human cannabinoid receptor 1 binding and activation of Cumyl-CBMICA and Cumyl-CBMINACA. *Drug Test Anal*. 2021;13(8):1499-1515. doi:10.1002/dta.3038

5. Pulver B, Schönberger T, Weigel D, et al. Structure elucidation of the novel synthetic cannabinoid Cumyl-Tosyl-Indazole-3-Carboxamide (Cumyl-TsINACA) found in illicit products in Germany. *Drug Test Anal*. Published online April 9, 2022. doi:10.1002/dta.3261

6. Pulver B, Riedel J, Schönberger T, et al. Comprehensive structural characterisation of the newly emerged synthetic cannabimimetics Cumyl-BC[2.2.1]HpMeGaClone, Cumyl-BC[2.2.1]HpMINACA, and Cumyl-BC[2.2.1]HpMICA featuring a norbornyl methyl side chain. *Forensic Chem*. 2021;26:100371. doi:10.1016/j.forc.2021.100371

7. Tsochatzis ED, Alberto Lopes J, Holland MV, Reniero F, Palmieri G, Guillou C. Identification and analytical characterization of a novel synthetic cannabinoid-type substance in herbal material in Europe. *Molecules*. 2021;26(4):793. doi:10.3390/molecules26040793

8. European Monitoring Centre for Drugs and Drug Addiction. *European Drug Report 2022: Trends and Developments.* Publications Office; 2022. Accessed June 20, 2022. https://data.europa.eu/doi/10.2810/75644

9. EMCDDA. European Database for New Drugs (EDND). Published 2022. Accessed January 18, 2022. https://ednd2.emcdda.europa.eu

10. Zaitsu K, Katagi M, Tsuchihashi H, Ishii A. Recently abused synthetic cathinones, α-pyrrolidinophenone derivatives: a review of their pharmacology, acute toxicity, and metabolism. *Forensic Toxicol*. 2014;32(1):1-8. doi:10.1007/s11419-013-0218-1

11. Chen Y, Canal CE. Structure–activity relationship study of psychostimulant synthetic cathinones reveals nanomolar antagonist potency of α-pyrrolidinohexiophenone at human muscarinic M $_2$ receptors. *ACS Chem Neurosci*. 2020;11(6):960-968. doi:10.1021/acschemneuro.0c00008

12. Taffe MA, Nguyen JD, Vandewater SA, Grant Y, Dickerson TJ. Effects of α-pyrrolidinophenone cathinone stimulants on locomotor behavior in female rats. *Drug Alcohol Depend*. 2021;227:108910. doi:10.1016/j.drugalcdep.2021.108910

13. Assi S, Gulyamova N, Kneller P, Osselton D. The effects and toxicity of cathinones from the users' perspectives: A qualitative study. *Hum Psychopharmacol Clin Exp*. 2017;32(3):e2610. doi:10.1002/hup.2610

14. Beck O, Bäckberg M, Signell P, Helander A. Intoxications in the STRIDA project involving a panorama of psychostimulant pyrovalerone derivatives, MDPV copycats. *Clin Toxicol*. 2018;56(4):256-263. doi:10.1080/15563650.2017.1370097

15. Nóbrega L, Dinis-Oliveira RJ. The synthetic cathinone α-pyrrolidinovalerophenone (α-PVP): pharmacokinetic and pharmacodynamic clinical and forensic aspects. *Drug Metab Rev*. 2018;50(2):125-139. doi:10.1080/03602532.2018.1448867

16. Dargan PI, Sedefov R, Gallegos A, Wood DM. The pharmacology and toxicology of the synthetic cathinone mephedrone (4-methylmethcathinone). *Drug Test Anal*. 2011;3(7-8):454-463. doi:10.1002/dta.312

17. Coppola M, Mondola R. 3,4-Methylenedioxypyrovalerone (MDPV): Chemistry, pharmacology and toxicology of a new designer drug of abuse marketed online. *Toxicol Lett*. 2012;208(1):12-15. doi:10.1016/j.toxlet.2011.10.002

18. Simmler L, Buser T, Donzelli M, et al. Pharmacological characterization of designer cathinones in vitro. *Br J Pharmacol*. 2013;168(2):458-470. doi:10.1111/j.1476-5381.2012.02145.x

19. Eshleman AJ, Wolfrum KM, Reed JF, et al. Structure-Activity Relationships of Substituted Cathinones, with Transporter Binding, Uptake, and Release. *J Pharmacol Exp Ther*. 2017;360(1):33-47. doi:10.1124/jpet.116.236349

20. Bundesgesetzblatt [2016] Teil I: Nr. 55: S.2615. Gesetz zur Bekämpfung der Verbreitung neuer psychoaktiver Stoffe. Published November 21, 2016. Accessed September 25, 2020. http://www.bgbl.de/xaver/bgbl/start.xav?startbk=Bundesanzeiger_BGBl&jumpTo=bgbl116s2615.pdf

21. Bundesgesetzblatt [2021] Teil I: Nr. 38: S.2231. Zweite Verordnung zur Änderung der Anlage des Neue-psychoaktive-Stoffe-Gesetzes. Published July 2, 2021. Accessed May 27, 2022. http://www.bgbl.de/xaver/bgbl/start.xav?startbk=Bundesanzeiger_BGBl&jumpTo=bgbl121s2231.pdf

22. NpSG - Neue-psychoaktive-Stoffe-Gesetz. Accessed June 22, 2022. https://www.gesetze-im-internet.de/npsg/BJNR261510016.html

23. Pulver B, Fischmann S, Westphal F, et al. The ADEBAR project: European and international provision of analytical data from structure elucidation and analytical characterization of NPS. *Drug Test Anal*. Published online May 24, 2022:dta.3280. doi:10.1002/dta.3280

24. EMCDDA. *EWS Formal Notification 3,4-Pr-PipVP*. European Monitoring Centre for Drugs and Drug Addiction; 2022:3. Accessed September 14, 2022. https://ednd2.emcdda.europa.eu/ednd/management/resources/download/2456ee8-ednd

25. van Den Dool H, Dec. Kratz P. A generalization of the retention index system including linear temperature programmed gas—liquid partition chromatography. *J Chromatogr A*. 1963;11:463-471. doi:10.1016/S0021-9673(01)80947-X

26. checkit Warnungen 2022 KW9. Aktuelle Warnungen und besondere Ergebnisse. Published March 4, 2022. Accessed June 22, 2022. https://checkit.wien/media/checkit_Warnungen_2022_KW9.pdf

27. Yovanovich AC, Goodpaster JV, Minto RE. Identification of 1-(2,3-dihydro-1H-inden-5-yl)-2-(ethylamino)pentan-1-one (bk-IVP) in a seized drug exhibit. *J Forensic Sci*. 2018;63(3):915-920. doi:10.1111/1556-4029.13642

28. SWGDRUG. *SWGDRUG Recommendations*. Scientific Working Group for the Analysis of Seized Drugs (SWGDRUG); 2019. Accessed March 9, 2022. https://www.swgdrug.org/Documents/SWGDRUG%20Recommendations%20Version%208_FINAL_ForPosting_092919.pdf

29. Mcluckey SA, Goeringer DE. SPECIAL FEATURE: TUTORIAL Slow Heating Methods in Tandem Mass.

30. Mitchell Wells J, McLuckey SA. Collision-Induced Dissociation (CID) of Peptides and Proteins. In: *Methods in Enzymology*. Vol 402. Elsevier; 2005:148-185. doi:10.1016/S0076-6879(05)02005-7

31. Błażewicz A, Bednarek E, Popławska M, Olech N, Sitkowski J, Kozerski L. Identification and structural characterization of synthetic cathinones: N-propylcathinone, 2,4-dimethylmethcathinone, 2,4-dimethylethcathinone, 2,4-dimethyl-α-pyrrolidinopropiophenone, 4-bromo-α-pyrrolidinopropiophenone, 1-(2,3-dihydro-1H-inden-5-yl)-2-(pyrrolidin-1-yl)hexan-1-one and 2,4-dimethylisocathinone. *Forensic Toxicol*. 2019;37(2):288-307. doi:10.1007/s11419-018-00463-w

32. Tyler Davidson J, Piacentino EL, Sasiene ZJ, et al. Identification of novel fragmentation pathways and fragment ion structures in the tandem mass spectra of protonated synthetic cathinones. *Forensic Chem*. 2020;19:100245. doi:10.1016/j.forc.2020.100245

33. Bellamy LJ. *The Infrared Spectra of Complex Molecules: Volume Two Advances in Infrared Group Frequencies*. Springer Netherlands; 1980. Accessed November 10, 2021. https://doi.org/10.1007/978-94-011-6520-4

34. Socrates G. *Infrared and Raman Characteristic Group Frequencies: Tables and Charts*. 3rd ed. Wiley; 2001.

35. Hesse M, Meier H, Zeeh B, Bienz S, Bigler L, Fox T. *Spektroskopische Methoden in der organischen Chemie*. 8. überarbeite und erweiterte Auflage. Georg Thieme Verlag; 2012.

36. Lin-Vien D, ed. *The Handbook of Infrared and Raman Characteristic Frequencies of Organic Molecules*. Academic Press; 1991.

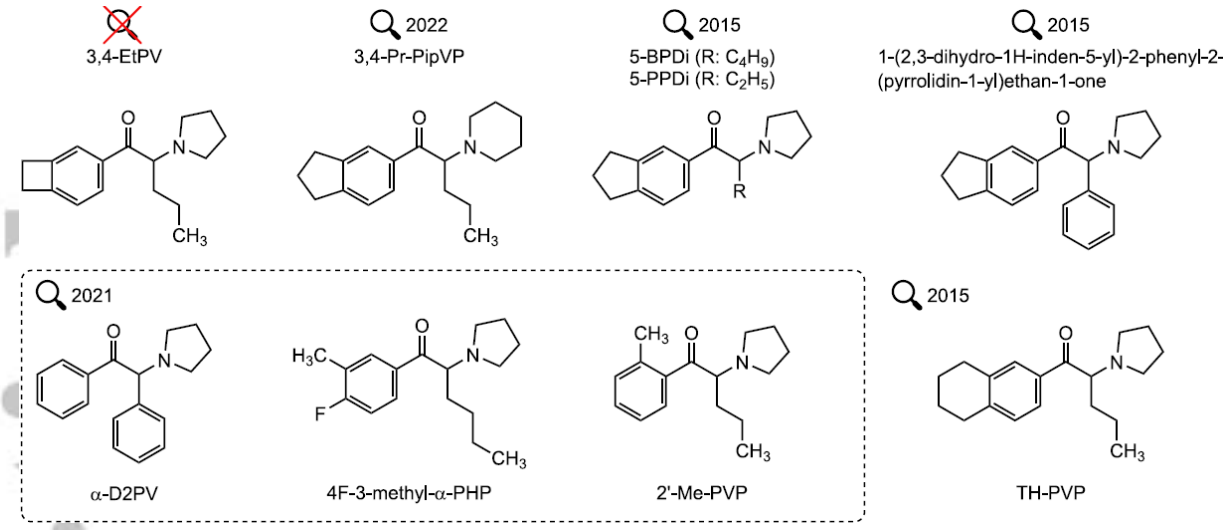

Figure 1: Molecular structures of 3,4-EtPV and 3,4-Pr-PipVP. The structural analog 5-BPDi (top), and the three pyrrolidine-type synthetic cathinones notified to the EMCDDA in 2021 for the first time are also shown (bottom).

Compounds derived from 2-phenylethylamines

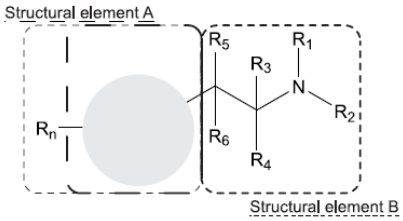

Compounds with a base structure derived from 2-phenylethan-1-amine with a molecular weight of less than 500 u and with a molecular structure composed of the structural elements A and B and their substitutents are included in the generic definition of the German NpSG.

Structural element A	The following ring systems are defined as possible structural elements A: Phenyl-, naphthyl-, tetralinyl-, methylenedioxyphenyl-, ethylenedioxyphenyl-, furyl-, pyrrolyl-, thienyl-, pyridyl-, benzofuranyl-, dihydrobenzofuranyl-, indanyl-, indenyl-, tetrahydrobenzodifuranyl-, benzodifuranyl-, tetrahydrobenzodipyranyl-, cyclopentyl-, cyclohexyl-.
Substitution of structural element A	The ring systems of structural element A may be substituted at any position with the following atoms or atomic groups (R_n): Hydrogen, fluorine, chlorine, bromine, iodine, alkyl (up to C_6), alkenyl (up to C_6), alkinyl (up to C_6), alkoxy (up to C_6), carboxy, alkylsulfanyl (up to C_6) and nitro group.
Further modification of R_n	R_n can further be substituted with any chemically possible combinations of the elements: carbon, hydrogen, nitrogen, oxygen, sulfur, fluorine, chlorine, bromine and iodine. The substituents formed in this way may have a maximum continuous chain length of eight atoms (not counting hydrogen atoms and atoms of ring structures). If R_n yields cyclic systems fused to the structural element A, they are not included in the definition of the substance group.
Structural element B	The 2-aminoethyl side chain of structural element B may be substituted by R_1 to R_6:
R_1, R_2	Hydrogen, alkyl (up to C_6), cycloalkyl (up to C_6), benzyl, alkenyl (up to C_6), alkinyl (up to C_6), alkylcarbonyl (up to C_6), hydroxy and amino groups. Also included are substances in which the nitrogen atom is part of a cyclic system (for example, pyrrolidinyl-, piperidinyl-). Further modification of R_1 and R_2 like R_n but with a maximum continuous chain length of ten atoms.
R_3, R_4, R_5, and R_6	Hydrogen, fluorine, chlorine, bromine, iodine, alkyl (up to C_{10}), cycloalkyl (up to C_{10}), benzyl, phenyl, alkenyl (up to C_{10}), alkinyl (up to C_{10}), hydroxy, alkoxy (up to C_{10}), alkylsulfanyl (up to C_{10}), alkyloxycarbonyl groups (up toC_{10}), including chemical compounds in which substitutions lead to a ring closure with the structural element A or to ring systems containing the radicals R_3 to R_6. These ring systems may contain four to six atoms. Further modification of R_1 and R_2 like R_n but with a maximum continuous chain length of twelve atoms.

Figure 2: Simplified overview of the section of the annex to the German NpSG (Anlage des Neue-psychoaktive-Stoffe-Gesetzes published on November 21, 2016 (Federal Law Gazette I p. 2615), last amended by Article 1 of the Act of July 02, 2021 (Federal Law Gazette I p. 2231)) that generically defines the phenylethylamines. This translation of the German legislative text in the official document[22] is not binding and has no legal effect for compliance or enforcement purposes.

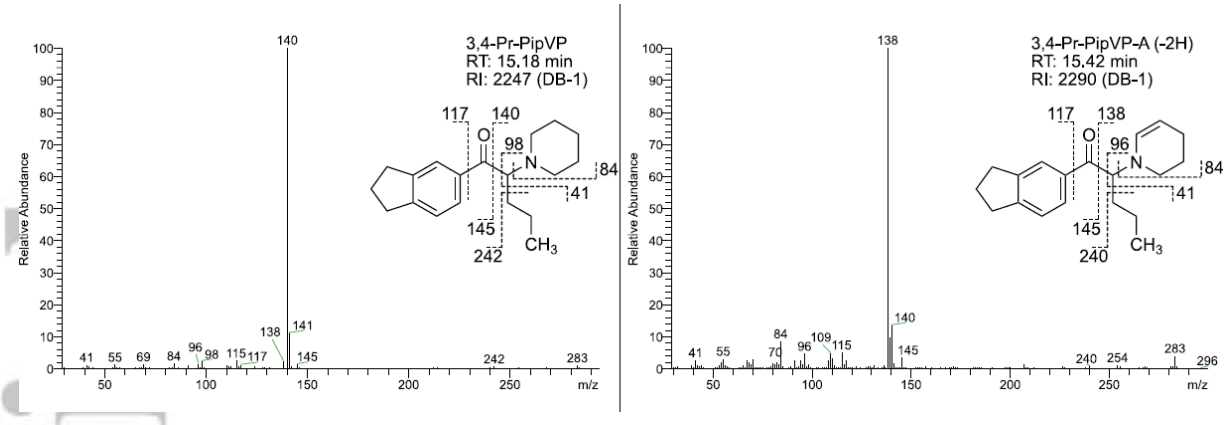

Figure 3: EI mass spectra of 3,4-Pr-PipVP (left) and the GC-artifact produced upon injection into the liner (right) together with proposed molecular structures of the observed fragment ions. The position of the double bond within the ring remains uncertain.

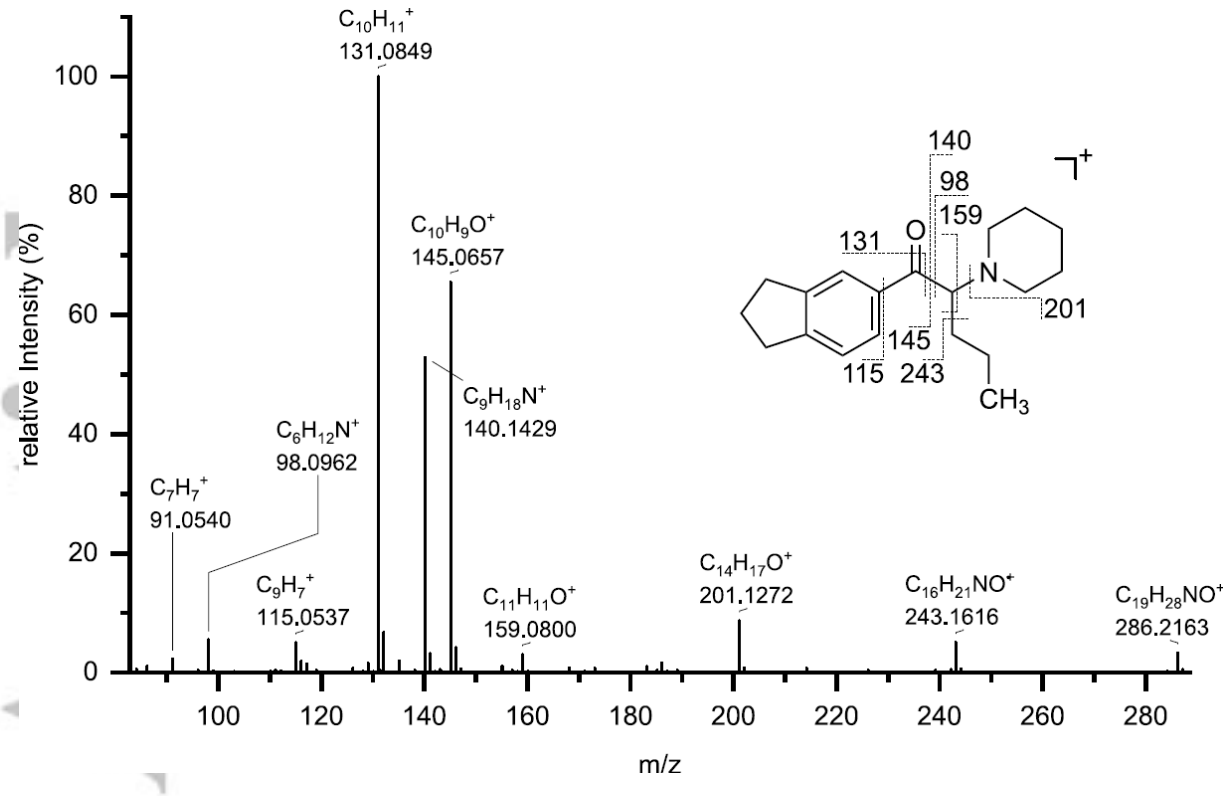

Figure 4: HR-ESI-MS/MS (40 eV) mass spectrum of 3,4-Pr-PipVP and proposed fragmentation of the protonated precursor ion.

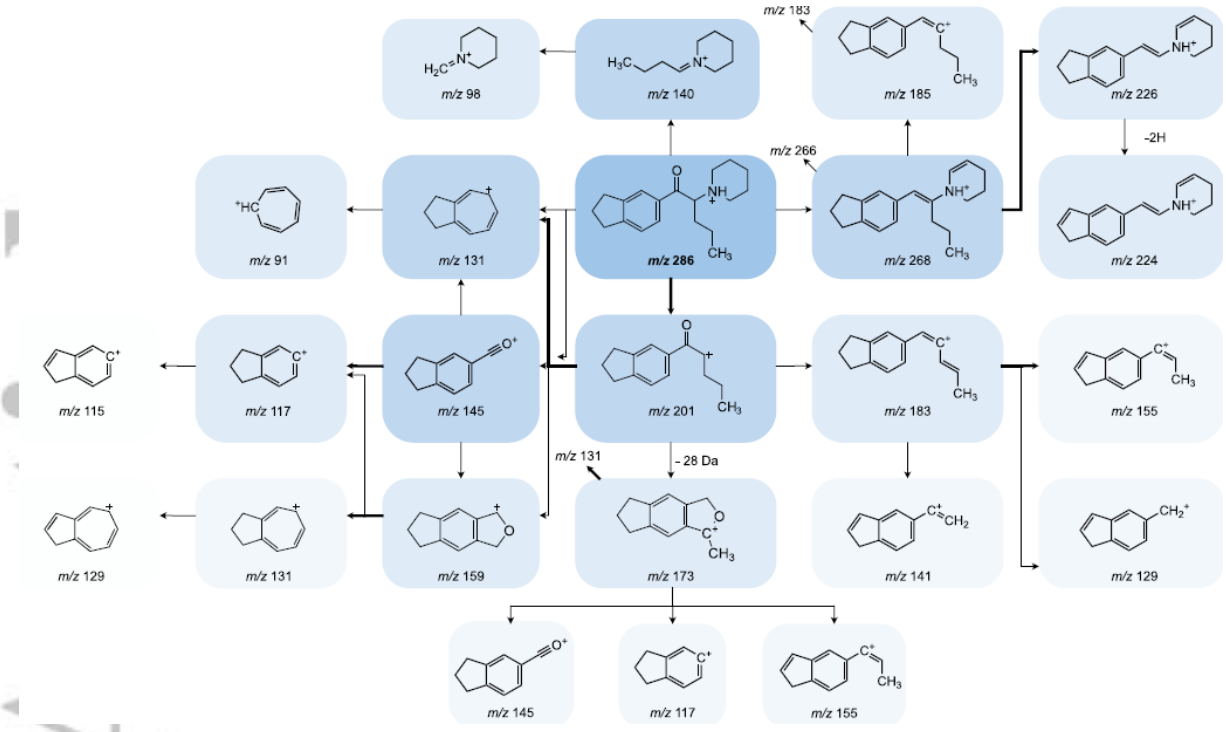

Figure 5: Proposed MS^n fragmentation pathway based on ESI-Q_{IT}-MS^n experiments and HR-MS/MS data of 3,4-Pr-PipVP (bold). A lower tint indicates increasing MS^n stages, and bold arrows indicate the base peak in the respective MS^n mass spectra.

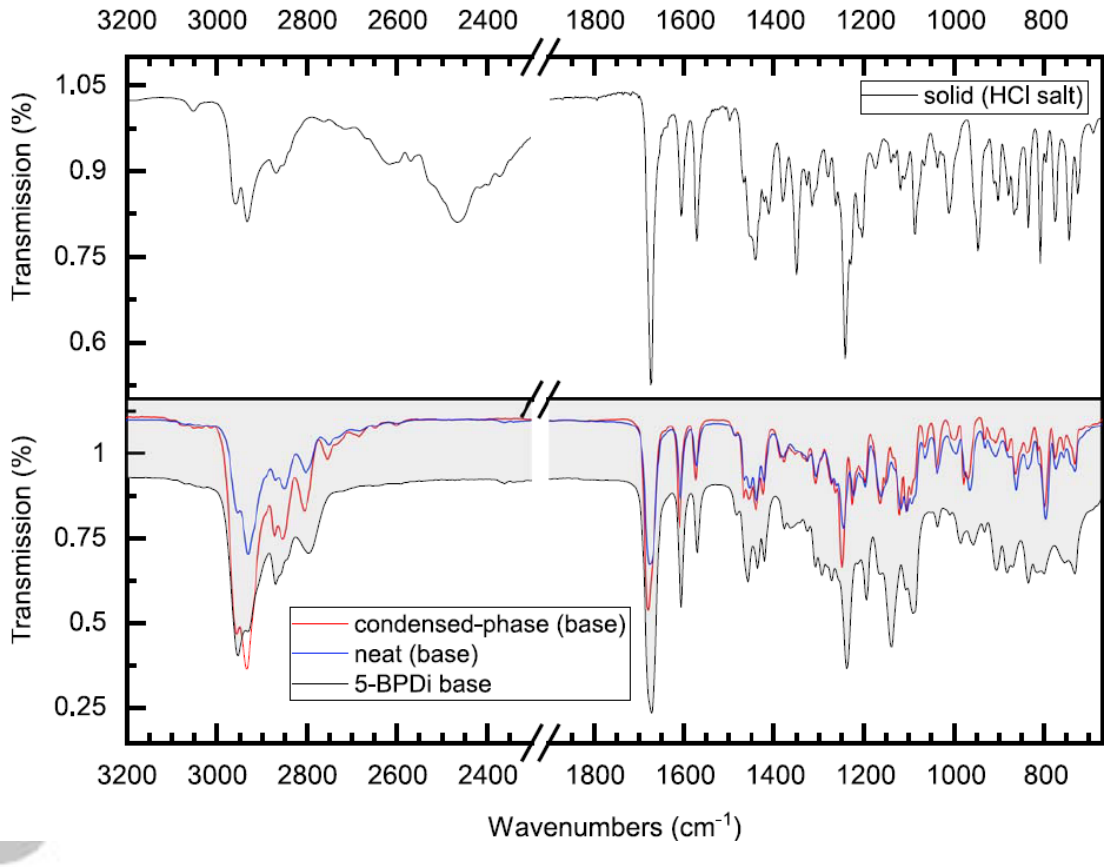

Figure 6: Infrared spectra of 3,4-Pr-PipVP as hydrochloride (top) and free base (bottom). Neat film (bottom, blue) and condensed-phase IR spectra (bottom, red) of 3,4-Pr-PipVP are overlayed and compared to the IR spectrum of the free base form of 5-BPDi.

Table 1: Measured *m/z* values using HR-ESI-QToF-MS/MS, suggested ion formula, calculated *m/z* values, relative intensities, and mass error values of 3,4-Pr-PipVP and its fragment ions.

Ion type	**Measured *m/z***	**Relative Intensity %**	**Suggested Ion Formula**	**Calculated *m/z***	**Mass error [ppm]**
$[M+H]^+$	286.2163	3.3	$C_{19}H_{28}NO^+$	286.2165	0.7
$[M-H_2O+H]^+$	268.2063	0.1	$C_{19}H_{26}N^+$	268.2060	1.1
$[M-C_3H_7^{\bullet}+H]^{\bullet+}$	243.1616*	5.1	$C_{16}H_{21}NO^{\bullet+}$	243.1618	0.8
$[M-C_3H_7-H_2O]^+$	226.1591	0.4	$C_{16}H_{20}N^+$	226.159	0.4
$[M-C_3H_7-H_2-H_2O]^+$	224.1434	0.1	$C_{16}H_{18}N^+$	224.1434	<0.1
$[M-C_5H_{10}N]^+$	201.1272	8.7	$C_{14}H_{17}O^+$	201.1274	1.0
$[M-C_5H_{10}N-H_2O]^+$	185.1323	0.4	$C_{14}H_{17}^+$	185.1325	1.1
Fragment	183.1163	1	$C_{14}H_{15}^+$	183.1168	2.7
Fragment	173.1312*	0.5	$C_{13}H_{17}^+$	173.1325	7.5
Fragment	173.0959	0.7	$C_{12}H_{13}O^+$	173.0961	1.2
Fragment	159.0802	4	$C_{11}H_{11}O^+$	159.0804	1.3
Fragment	155.0854	1.1	$C_{12}H_{11}^+$	155.0855	0.6
Fragment	145.0657	65.5	$C_{10}H_9O^+$	145.0648	6.2
Alkyl piperidinyl	140.1429	52.9	$C_9H_{18}N^+$	140.1434	3.6
Fragment	131.0849	100	$C_{10}H_{11}^+$	131.0855	4.6
Fragment	117.0693	0.8	$C_9H_9^+$	117.0699	5.1
Fragment	129.0693	1.6	$C_{10}H_9^+$	129.0699	4.6
Fragment	116.0611*	0.9	$C_9H_8^{\bullet+}$	116.0621	8.6
Fragment	115.0537	5	$C_9H_7^+$	115.0542	4.3
Piperidinyl iminium	98.0962	5.5	$C_6H_{12}N^+$	98.0964	2.0
Tropylium ion	91.054	2.3	$C_7H_7^+$	91.0542	2.2

*only detected using the QToF instrument

Table 2: ^{13}C and ^{1}H NMR signals for 3,4-Pr-PipVP in DMSO-d_6 at 125 and 500 MHz, respectively.

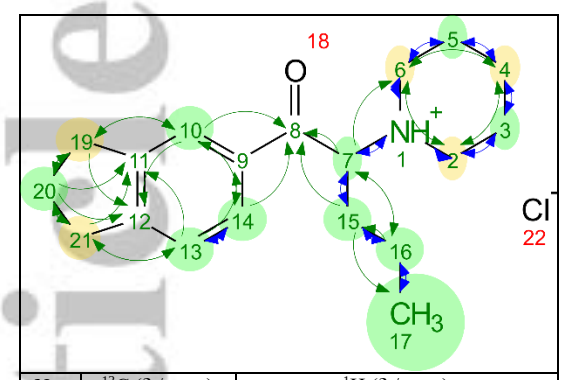

No.	^{13}C (δ / ppm)	^{1}H (δ / ppm)
1	-	10.12 (s, 1H)
2	50.25	3.04 (m, 1H), 3.61 (d: 11.92 Hz, 1H)
3	21.96	1.86 (m, 2H)
4	21.61	1.41, 1.68 (m, 2H)
5	21.96	1.86 (m, 2H)
6	51.83	3.07 (m, 1H), 3.27 (d: 12.19 Hz, 1H)
7	65.95	5.34 (m, 1H)
8	196.05	-
9	133.76	-
10	124.91	8.00 (s, 1H)
11	144.73	-
12	152.25	-
13	124.5	7.47 (d: 7.90 Hz, 1H)
14	127.48	7.93 (dd: 7.89, 1.75 Hz, 1H)
15	29.58	1.86 (m, 2H)
16	17.51	1.11 (m, 2H)
17	13.7	0.8 (t: 7.27 Hz, 3H)
18	-	-
19	31.84	2.96 (t: 7.51 Hz, 2H)
20	24.66	2.08 (p: 7.48 Hz, 2H
21	32.51	2.96 (t: 7.51 Hz, 2H)

Note: The arrows added to the molecule show the correlations based on the evaluations of the H, H-COSY (blue), and HMBC (green) spectra. The rough classification of the multiplicities and the approximate coupling constants are listed for the signals of the ^{1}H spectrum, as far as they could be determined.

Graphical Abstract

A new synthetic cathinone: 3,4-EtPV or 3,4-Pr-PipVP? An unsuccessful attempt to circumvent the German legislation on new psychoactive substances

Benedikt Pulver,
Jan Riedel,
Folker Westphal,
Steven Luhn,
Torsten Schönberger,
Jan Schäper,
Volker Auwärter,
Anton Luf,
Michael Pütz*

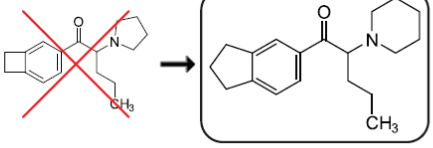

3,4-EtPV 3,4-Pr-PipVP

The failed synthesis of 3,4-EtPV highlights the ongoing efforts to deliberately circumvent generic definitions, which is increasingly difficult to achieve. 3,4-Pr-PipVP, identified in two samples (unintentionally?) mislabeled and advertised as '3,4-EtPV', is already scheduled under the German NpSG.